Excimer laser manipulation and pattering of gold nanoparticles on the SiO_2/Si surface

D.-Q. Yang, M. Meunier, and E. Sacher[a)]
Laboratoire de Procédés Laser, Groupe des Couches Minces and Département de Génie Physique, Ecole Polytechnique C.P. 6079, succursale Centre-Ville, Montréal, Québec H3C 3A7, Canada

(Received 29 October 2003; accepted 4 February 2004)

Au nanoparticles were deposited onto SiO_2/Si by evaporation, after which x-ray photoelectron spectroscopy (XPS) indicated some interfacial interaction between the Au and the Si. The sample was then processed by KrF pulsed excimer laser radiation (248 nm) in air, at a fluence of ~20 mJ/cm^2. Following this laser irradiation, XPS indicated the loss of substrate/nanoparticle interaction, resulting in the loss of cluster adhesion to the substrate and the formation of larger, isolated, spherical Au particles through rapid cluster coalescence. UV-visible spectral measurements indicated the absence of a surface plasmon resonance peak before irradiation, due to the small nanoparticle size (<3 nm); however, such a peak appeared at ~550 nm after irradiation, when the particle size increased to ~5.5 nm. Using 200-mesh transmission electron microscope grids as irradiation masks, we obtained Au nanoparticles in the unpatterned areas after irradiation. Such Au nanoparticle patterning may be used in biomolecular detector-based plasmon image-type sensors.
 [DOI: 10.1063/1.1689751]

INTRODUCTION

The size- and shape-dependent optical properties of Au nanoparticle have been of interest from both fundamental and applications points of view. One important property of Au nanoparticles is their surface plasmon resonance (SPR) in the visible spectral region, which has been used for surface-enhanced Raman spectroscopy and SPR detectors in biomolecular systems. However, the SPR spectra depend on particle size and shape, their interactions, the dielectric environments, etc.[1] One may, in fact, tune the SPR spectra by controlling one or more of these dependences.

There has recently been an increasing interest in the laser processing of nanoparticles. These processes include the reduction of the size[2–4] and the change of shape[5,6] of noble-metal nanoparticles through the nano- or femtosecond laser irradiation of larger particles suspended in aqueous solution. In addition lasers were employed to form smaller, spherical nanoparticles from larger supported particles, by using two different wavelengths of radiation, in vacuum or air;[7,8] this reduction of noble-metal nanoparticle size is explained in terms of a heat rise and melting, on excitation of the strong surface plasmon transition by the laser (e.g., Nd:YAG at 532 nm, which is close to the Au plasmon peak) in these studies.

We recently developed a treatment process similar to that presented here, but using low-energy, rare-gas, ion-beam irradiation to manipulate supported nanoparticles. Such manipulation was used to form nanostructures on *nonreactive* substrate surfaces.[9,10] The low-energy ion beam may also cause substrate surface damage. For these reasons, an alternative process would be desirable for circumstances requiring it.

[a)]Electronic mail: edward.sacher@polymtl.ca

EXPERIMENT

Here, we use a KrF pulsed excimer laser ($\lambda = 248$ nm) to irradiate supported Au particles on plasma-oxidized Si (SiO_2/Si) surfaces. Generally, evaporated Au atoms that are deposited on such surfaces form clusters[10–12] through surface diffusion and nucleation; as we shall mention later, and more fully discuss in a future paper, x-ray photoelectron spectroscopy (XPS) indicates a weak interaction at the Au/SiO_2 interface. The initial stage of Au deposition (e.g., a few monolayers), often results in nanoparticles shaped like prolate spheroids, which sometimes touch, and have a broad size distribution, reaching ±30%–50% of the mean cluster diameter.[13]

We used *n*-type Si wafers, cleaned with ethanol and dried in a stream of high-purity N_2 before treatment in an O_2 plasma at 5×10^{-2} Torr and 100 W of power for 2 min. This removes the native oxide and forms a new layer of SiO_2 on the surface: Fourier transform infrared spectra (not shown) indicated the loss of both adsorbed water and carbon contaminant present in the native oxide. The subsequent deposition of Au was performed *in situ*, at a base pressure of 1×10^{-7} Torr and a rate of 0.1 nm/s, by using an electron-beam evaporator. Laser irradiation was carried out in air, using a KrF excimer pulsed laser (GSI Lumonics, Inc., PulseMaster™ PM-800, $\lambda = 248$ nm, operating at a frequency of 20 Hz with a 20 ns pulse width at half-maximum). Contact-mode atomic force microscopy (AFM) was carried out on a Digital Multimode scanning probe microscope; commercially available silicon nitride cantilevers, with spring constants of 0.5 N m^{-1}, typical tip radii of 10–20 nm and tip half-angles of 35°, were used. The tip-scanning rate was 2 Hz, and 512 lines were used per image.

For these measurements, the integral gain was set at 2 V, the proportional gain was set at 3 V, and the deflection set

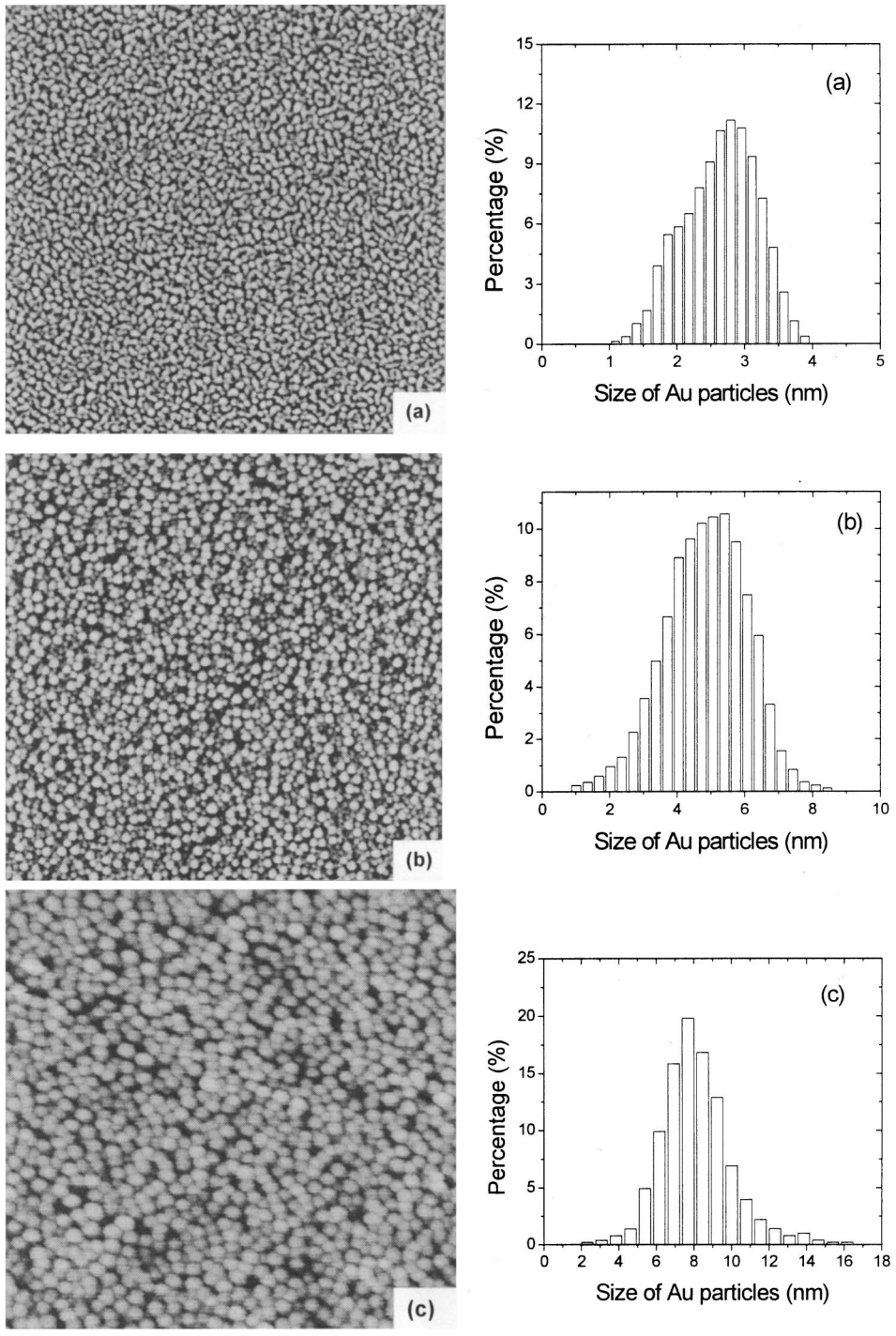

FIG. 1. Contact-mode AFM images of Au nanoparticles deposited onto the SiO_2/Si surface by evaporation. (a) As deposited, with a mean height of ~2.9 nm and a size distribution of 0.7. (b) After 30 laser pulses, with a mean height ~5.4 nm and a size distribution of 0.5. (c) After 200 pulses, with a mean height of 7.8 nm and a size distribution of 0.33. The image scales of (a) and (b) are 1 μm×1 μm, and that of (c) is 0.5×0.5 μm.

point (the contact pressure) was set at 0 V. After laser irradiation, we used a −1 V set point (attractive) for imaging, to avoid problems due to weak Au nanoparticle/substrate adhesion.

RESULTS AND DISCUSSION

Figure 1 shows the AFM surface morphologies and particle size distributions before [Fig. 1(a)] and after 30 [Fig. 1(b)] and 200 [Fig. 1(c)] laser pulses; size distributions were determined from particle heights. Clearly, nonspherical island-like particles are initially formed [Fig. 1(a)] on the SiO_2 surface, with a mean particle height of ~2.9 nm. After 30 pulses of laser irradiation [Fig. 1(b)], the nanoparticles were seen to have become well-defined, monodisperse, and spherical, with a mean height of ~5.4 nm; after 200 pulses [Fig. 1(c)], the mean height was ~7.8 nm. The measured relative size distributions, determined as the full width at half-maximum of the size distribution divided by the average

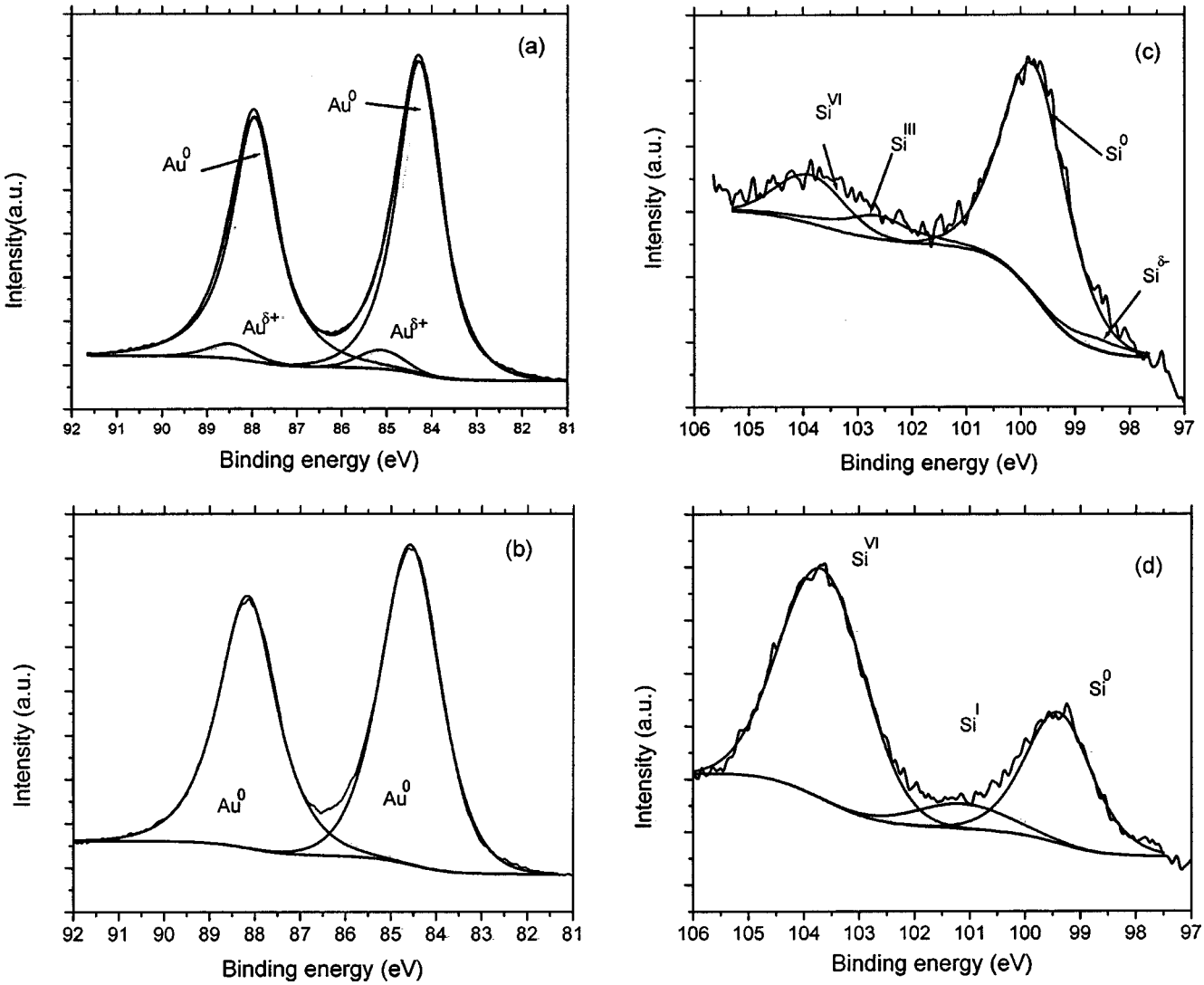

FIG. 2. XPS spectra of laser-processed Au nanoparticles: Au $4f$ (a) before treatment and (b) after treatment; Si $2p$ (c) before treatment and (d) after treatment.

size, given above, are 0.7 [Fig. 1(a)], 0.5 [Fig. 1(b)], and 0.33 [Fig. 1(c)], clearly indicating the dependence of the size distribution on the number of laser pulses.

High-resolution XPS Si $2p$ spectra (from the substrate) and Au $4f$ spectra (from the particles), show evidence of interaction before irradiation, in that a small (5%) Au $4f_{7/2}$ peak from $Au^{\delta+}$ is seen at 85.1 eV [Fig. 2(a)] and a small (5%) Si $2p$ peak from $Si^{\delta-}$ is seen at 98.6 eV [Fig. 2(c)]. These peaks are absent following irradiation [Figs. 2(b) and 2(d)]. It would thus appear that the formation of the larger particles on irradiation involves the loss of chemical interfacial interactions. The increase in Si $2p$ intensity on laser treatment [cf. Figs. 2(c) and 2(d)] is due to a decrease in Au cluster coverage, due to cluster growth and, possibly, to some loss of Au during laser irradiation.

The loss of Au/substrate interaction on laser irradiation results in a reduction in substrate adhesion. This is seen in Fig. 3, in which the AFM image, obtained at a set point of -1 V (because of the reduced adhesion), shows that the image center had previously been swept clean by *one scan* at a higher set-point value of 5 V; as we previously demonstrated,[14] contact-mode AFM, at a moderate set-point value, can be used to locally clean nanoclusters having weak adhesion. By comparison, we could not sweep Au clusters on the as-deposited sample, even at higher set-point values. Thus, laser irradiation may be used to locally clean such nanoparticles from surfaces.

UV-visible reflection spectra of the Au nanoparticles are found in Fig. 4. We see that SPR peaks are weakly observed for our as-deposited Au nanoparticles, due to their small size ($\sim$3 nm); however, after laser irradiation, a far stronger SPR peak appears around 550 nm from the larger sized ($\sim$5.5 nm) nanoparticles. The reduction in reflectivity above 550 nm, following laser treatment, may be due to a change in surface coverage and/or a change in particle morphology.

Using 200-mesh transmission electron microscope (TEM) grids as irradiation masks, we obtained the patterned Au nanoparticle image found in Fig. 5. The patterns are clearly distinguished, due to different nanoparticle sizes, shapes, and coverage on the SiO_2 surface. The presence of SPR, subsequent to treatment, strongly suggests that the Au nanoparticles in the untreated portion of the pattern (where the mobile nanoparticles diffuse and coalesce) gives rise to the SPR signal. Such patterning may be useful in creating

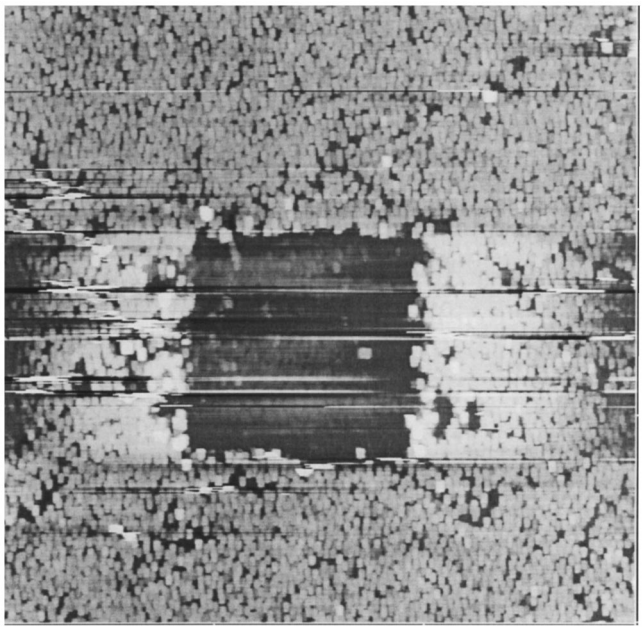

FIG. 3. Contact-mode AFM image of Au nanoparticles after laser processing (scale, 3 μm$\times$3 μm). The center of the image (1 μm$\times$1 μm) has been swept clean with one scan at a set-point value of 5 V. A set-point value of -1 V was used for AFM imaging. The Au nanoparticle have been removed in the region swept by the tip.

lab-on-a-chip biomolecular Au nanoparticle SPR sensors.

These experiments have shown that UV laser irradiation is strongly absorbed by the nanoparticles, increasing their kinetic energies and permitting enhanced diffusion and coalescence, as we also found for Ar^+ irradiation.[9] The absorption cross section of UV radiation increases as the particle size decreases (there is a d^{-3} dependence of the optical absorption cross section[1]), so that the smaller the Au nanoparticle, the greater the absorption cross section; this is complicated by the fact that the melting point of Au nanoparticles decreases with size,[15] leading to their disappearance. In fact, a strong UV light absorption cross-section may lead to the detachment of the initially formed Au/substrate adhesion.[16]

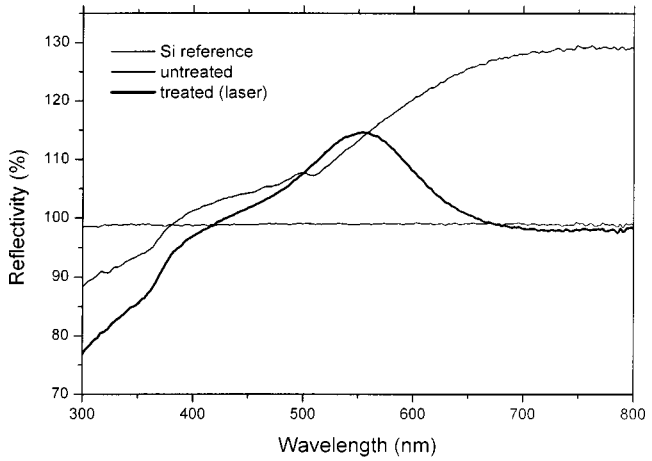

FIG. 4. A comparison of UV-visible reflection spectra of Au nanoparticles before and after laser processing. SiO_2/Si was referenced for comparison.

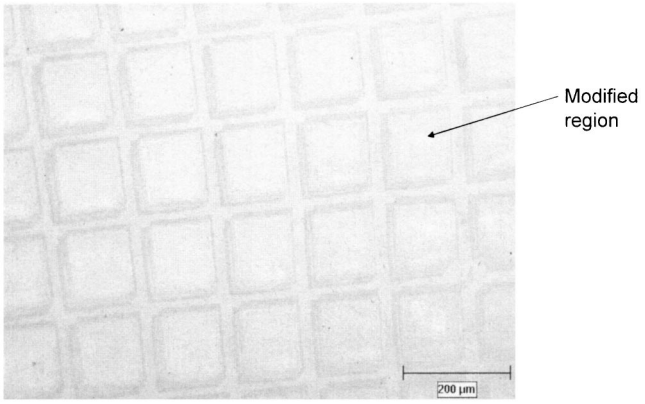

FIG. 5. Optical image of Au nanoparticles after laser patterning, using a TEM grid as a mask.

This loss of adhesion permits the nanoparticle to diffuse and coalesce on the substrate. As mentioned earlier, some Au may also be lost. Thus, as with Ar^+ irradiation, there may be a competition between treatment-induced loss and particle coalescence; we found that, for a give laser fluence, the stabilized Au nanoparticle dimension is reached within a relatively short irradiation time.[16]

CONCLUSIONS

In summary, we have demonstrated that the KrF pulsed excimer laser irradiation of Au nanoparticles provokes their loss of adhesion to the substrate, and their coalescence into larger, spherical nanoparticles; the treated nanoparticles show a SPR peak at ~550 nm. This treatment permits the formation of patterned Au nanoparticles, useful as biomolecular Au nanoparticle SPR sensors.

ACKNOWLEDGMENTS

We thank the Natural Sciences and Engineering Research Council of Canada for funding, and Dr. S. Bah for technical assistance on Au cluster deposition.

[1] U. Kreibig and M. Vollmer, *Optical Properties of Metal Clusters* (Springer, Berlin, 1995); K. L. Kelly, E. Coronado, L. L. Zhao, and G. C. Schatz, J. Phys. Chem. B **107**, 668 (2003).
[2] A. Takami, H. Yamada, K. Nakano, and S. Koda, Jpn. J. Appl. Phys. **35**, L781 (1996).
[3] H. Kurita, A. Takami, and S. Koda, Appl. Phys. Lett. **72**, 789 (1998).
[4] F. Mafune, J.-Y. Kohno, Y. Tkeda, and T. Kondow, J. Phys. Chem. B **105**, 9050 (2001).
[5] S. Link, C. Burda, M. B. Mohamed, B. Nikoobakht, and M. A. El-Sayed, J. Phys. Chem. B **103**, 1165 (1999).
[6] M. Kaempfe, T. Rainer, K. J. Berg, G. Seifert, and H. Graener, Appl. Phys. Lett. **74**, 1200 (1999); J. Phys. Chem. B **104**, 11874 (2000).
[7] J. Bosbach, D. Martin, F. Stietz, T. Wenzel, and F. Träger, Appl. Phys. Lett. **74**, 2605 (1999).
[8] M. Kawasaki and M. Hori, J. Phys. Chem. B **107**, 6760 (2003).
[9] D.-Q. Yang, K. N. Piyakas, and E. Sacher, Surf. Sci. **536**, 67 (2003).
[10] D.-Q. Yang, E. Sacher, and M. Meunier (unpublished).
[11] A. A. Schmidt, H. Eggers, K. Herwig, and R. Anton, Surf. Sci. **349**, 301 (1996).
[12] K. Luo, D. Y. Kim, and D. W. Goodman, J. Mol. Catal. A: Chem. **167**, 191 (2001).
[13] H. Brune, Surf. Sci. Rep. **31**, 121 (1998).
[14] D.-Q. Yang and E. Sacher, Appl. Surf. Sci. **210**, 158 (2003).
[15] Ph. Buffat and J.-P. Borel, Phys. Rev. A **13**, 2287 (1976).
[16] D.-Q. Yang, M. Meunier, and E. Sacher (unpublished).